Journal of Statistical Mechanics: Theory and Experiment
An IOP and SISSA journal

Self-organization without conservation: are neuronal avalanches generically critical?

Juan A Bonachela, Sebastiano de Franciscis, Joaquín J Torres and Miguel A Muñoz

Departamento de Electromagnetismo y Física de la Materia and Instituto de Física Teórica y Computacional Carlos I, Facultad de Ciencias, Universidad de Granada, 18071 Granada, Spain
E-mail: jabonachela@onsager.ugr.es, sebast@onsager.ugr.es, jtorres@onsager.ugr.es and mamunoz@onsager.ugr.es

Received 4 December 2009
Accepted 18 January 2010
Published 18 February 2010

Online at stacks.iop.org/JSTAT/2010/P02015
doi:10.1088/1742-5468/2010/02/P02015

Abstract. Recent experiments on cortical neural networks have revealed the existence of well-defined *avalanches* of electrical activity. Such avalanches have been claimed to be generically scale invariant—i.e. power law distributed—with many exciting implications in neuroscience. Recently, a self-organized model has been proposed by Levina, Herrmann and Geisel to explain this empirical finding. Given that (i) neural dynamics is dissipative and (ii) there is a loading mechanism progressively 'charging' the background synaptic strength, this model/dynamics is very similar in spirit to forest-fire and earthquake models, archetypical examples of non-conserving self-organization, which have recently been shown to lack true criticality. Here we show that cortical neural networks obeying (i) and (ii) are not generically critical; unless parameters are fine-tuned, their dynamics is either subcritical or supercritical, even if the pseudo-critical region is relatively broad. This conclusion seems to be in agreement with the most recent experimental observations. The main implication of our work is that, if future experimental research on cortical networks were to support the observation that truly critical avalanches are the norm and not the exception, then one should look for more elaborate (adaptive/evolutionary) explanations, beyond simple self-organization, to account for this.

Keywords: phase transitions into absorbing states (theory), self-organized criticality (theory), self-organized criticality (experiment), neuronal networks (theory)

1742-5468/10/P02015+26$30.00

Contents

1. Introduction and outlook **2**
- 1.1. Generic scale invariance . . . 2
- 1.2. Scale invariance in neuronal avalanches? . . . 3
- 1.3. Goals and outlook . . . 5

2. The Levina–Herrmann–Geisel (LHG) model **5**

3. Model analysis **7**
- 3.1. The static limit . . . 7
- 3.2. The dynamic model . . . 8
  - 3.2.1. Numerical analyses. . . . 8
  - 3.2.2. Characterization of criticality. . . . 11

4. Analytical results **15**

5. A simple absorbing state Langevin equation approach **19**

6. Conclusions **20**

Acknowledgments **22**

Appendix: Synchronization and oscillatory properties **22**

References **24**

1. Introduction and outlook

1.1. Generic scale invariance

In contrast to what occurs for standard criticality, where a control parameter needs to be carefully tuned to observe scale invariance, certain phenomena such as earthquakes, solar flares, avalanches of vortices in type II superconductors, and rainfall, to name but a few, exhibit generic power laws—i.e. they lie generically at a critical point without any apparent need for parameter fine-tuning [1, 2]. Ever since the concept of *self-organized criticality* [1] was proposed to account for phenomena like these, it has generated a lot of excitement, and countless applications in almost every possible field of research have been developed. Establishing the necessary and sufficient conditions for a given system to self-organize to a critical point is still a key challenge.

In this context, it has been established from a general viewpoint that *conserving dynamics* (i.e. that in which some quantity is conserved throughout the system evolution) is a crucial ingredient in generating true self-organized criticality in slowly driven systems [3, 4]. In this way, non-conserving self-organized systems have been shown *not* to be truly scale invariant (see [4] and references therein). While sandpiles, rice piles, and other prototypical self-organized models are examples of conserving self-organizing systems, forest-fire and earthquake automata are two examples of non-conserving models. They were both claimed historically to self-organize to a critical point and they were both shown afterwards to lack true scale-invariant behavior (see [4] and references therein).

doi:10.1088/1742-5468/2010/02/P02015

J. Stat. Mech. (2010) P02015

The main reason for this is, in a nutshell, that non-conserving systems combine driving (loading) and dissipation, and this suffices to keep the system 'hovering around' a critical point separating an active from a quiescent or absorbing phase (driving slowly pushes the system into the active phase and dissipation takes it back to the absorbing phase). But in order to have the system lying exactly *at* the critical point one requires an exact cancelation between dissipation and driving (loading); such a perfect balance can only be achieved by parameter fine-tuning, and then the system cannot be properly called 'self-organized'.

This mechanism of (non-conserving) self-organization has been termed self-organized quasi-criticality (SOqC) [4] to underline the conceptual differences from truly scale-invariant, (conserving) self-organized criticality (SOC) [1, 2]. From now on, we will use the acronym SOqC to refer to non-conserving self-organized systems, and will keep the term SOC for self-organized conserved systems.

SOqC may explain the 'approximate scale invariance' (with apparent power law behavior extending for a few decades) observed in many real systems such as those mentioned above (earthquakes and forest fires) but, strictly speaking, it fails to explain true scale invariance. SOqC systems require some degree of parameter tuning to lie sufficiently close to criticality. For a much more detailed explanation of the SOqC mechanism and its differences from SOC, we refer the reader to [4].

1.2. Scale invariance in neuronal avalanches?

Neuronal avalanches were first reported by Beggs and Plenz, who analyzed *in vitro* cortical neural networks using slices of rat cortex as well as cultured networks [5]–[7]. More recently, neuronal avalanches have been observed also *in vivo* [8]. In all these cases, cortical neurons form dense networks which, under adequate conditions, are able to spontaneously generate electrical activity [9]. The associated *local field potentials* can be recorded by using multielectrode arrays [5]. Each electrode in the array monitors the electrical activity of a local group of neurons (which for convenience can be thought of as a unique 'effective' neuron; a review of the experimental techniques and methods involved can be found in [10]). According to Beggs and Plenz [5]–[7], activity appears in the form of 'avalanches', i.e. localized activity is generated spontaneously at some electrode and propagates to neighboring ones in a cascade process which occurs in a time duration much shorter (tens of milliseconds) than that of the quiescent periods between avalanches (typically of the order of seconds). Previous experimental research on cultured networks had identified the existence of spontaneously generated *synchronized bursts* of activity (involving synchronous activation of many neurons), followed by silent periods of variable duration [11]–[15] (theoretical work has been done to explain such a coherent or synchronous behavior; see, for instance, [16, 17]). The main breakthrough by Beggs and Plenz in [5] was to enhance the resolution and bring the internal structure of 'synchronized' bursting events to light. In other words, the apparently synchronous activation of many neurons required for a synchronized burst corresponds to a sequence of neuron activations, i.e., a neuronal avalanche, which generates spatio-temporal patterns of activation confined between two consecutive periods of quiescence.

Experimental measurements of avalanches can be performed, and the distribution of quantities such as (i) the avalanche size s (i.e. the number of electrodes at which a non-

J. Stat. Mech. (2010) P02015

vanishing signal is detected during an avalanche) and (ii) the avalanche lifetime, t, can be recorded. What is relevant for us here is that, according to Beggs and Plenz, avalanches seem to be generically scale invariant [5]–[7]; in particular, avalanche sizes, s, and times t are distributed as

$$P(s) \sim s^{-3/2}\mathcal{F}(s/s_c), \qquad P(t) \sim t^{-2}\mathcal{G}(t/t_c) \tag{1}$$

respectively, where $\mathcal{F}$ and $\mathcal{G}$ are two cut-off functions; the cut-off s_c grows in a scale-invariant way as a function of system size: the larger the system, the larger the cut-off, providing evidence for finite size scaling. The cut-off t_c appears at very small times, so the evidence for scale invariance is much stronger for s than for t.

These results have been claimed to be robust across days, samples, and pharmacological variations of the culture medium [5]–[7]. The exponent values in equation (1) coincide with their mean-field counterparts for avalanches in sandpiles (the prototypical examples of self-organized criticality) [18]. Mean-field exponents do not come as a surprise: given the highly entangled structure of the underlying network (which has been reported to have the *small-world property* [19]), mean-field behavior is to be expected for critical phenomena occurring on it [20].

Finally, recalling that, at a mean-field level, avalanche dynamics can be interpreted as a *branching process* [21], an empirical study of the branching ratio, σ (defined as the fraction of active electrodes per active electrode at the previous time bin), was performed in [5, 22]. It was found that the value of σ measured for avalanches starting from one single electrode is very close to unity, in agreement with the critical value of marginally propagating branching processes, $\sigma_c = 1$.

From these results, it has been claimed that cortical neural networks are generically critical, i.e. scale invariant, and that they reach such a critical state in a 'self-organized' way [5]. Scale invariance in the propagation of neural activity has raised a great deal of interest and excitement in neuroscience. For instance, critical neural avalanches have been claimed to lead to [12, 5]:

- optimal transmission and storage of information [5]–[7], [22, 23],
- optimal computational capabilities [24],
- large network stability [25],
- maximal sensitivity to sensory stimuli [26], etc.

Let us caution that discrepant results, i.e. non-critical neuronal avalanches, have also been recently reported in the literature. For instance, measurements of cortical local field potentials were performed by Bédard *et al* [27] using parietal cat cortex. None of the features reported by Beggs and Plenz [5] were observed for such a network; not only was the observed behavior not critical, but also it was not even possible to observe clean-cut avalanches. It was argued that the absence of scale-free avalanches could stem from fundamental differences between the cortex regions considered in [27] and in [5]. Moreover, in a recent review paper, Pasquale *et al* [28] report on different empirical kinds of avalanche distributions: critical, subcritical, or supercritical, depending on various factors. These authors conclude that critical avalanches can indeed emerge, but they are more the exception that the rule.

J. Stat. Mech. (2010) P02015

1.3. Goals and outlook

The main goal of this paper is to elucidate from a theoretical viewpoint whether neuronal avalanches are truly critical or not. Or, more precisely, to understand whether self-organizing mechanisms (such as those of SOC or SOqC) can explain the findings for neuronal avalanches. To this end, we rely extensively on a model for neuronal avalanches proposed recently by Levina, Herrmann and Geisel [29]. The model is a self-organized one, including integrate-and-fire neurons and short-term synaptic plasticity. It has been claimed, both analytically and numerically, to back the existence of generically (strictly) critical neuronal avalanches in a very broad region of parameter space [29].

The key observation which motivated the present work is the fact that local conservation laws, such as those required to have truly critical self-organized (SOC) behavior, are not present for neural networks in any obvious way. If cortical networks are represented as an electrical circuit, perfect transmission without loss of energy is an unrealistic idealization and, analogously, if they are modeled as networks of dynamical synapses, there also exist dissipative or 'leakage' phenomena. In summary, *no quantity is strictly conserved in neural signal transmission*. Reasonably enough, the Levina, Herrmann and Geisel (LHG) model [29] is also a non-conserving one (see below).

Therefore, the existence of critical neuronal avalanches (both experimentally and in the LHG model) seems to be in contradiction with the general conclusion in [4], i.e. the lack of true criticality in non-conserving systems. In this way, a rationalization of neuronal avalanches would only be possible, at best, in terms of self-organized *quasi-criticality* (SOqC), and not in terms of *strict criticality* as suggested in [29].

Following the steps in [4], here we shall underline the analogies and differences between the model given by Levina *et al* and other non-conserving self-organized models such as those for earthquakes or forest fires. We shall show that the LHG model is *not* generically critical: it can be critical, subcritical or supercritical depending on parameter values; fine-tuning is required to achieve strict scale invariance. Still, the model is capable of generating, for a relatively wide parameter range, pseudo-critical avalanches with associated truncated power laws which can suffice to explain empirical observations.

This conclusion—i.e. the lack of true criticality—is expected to apply not only to the model of [29], but also to empirical neuronal avalanches. It suggests that if neuronal avalanches turned out to be truly critical, the ultimate reason for that should be looked for in some type of adaptive/evolutionary mechanism [30] or in homeostatic processes [31], but cannot be generically ascribed to plain self-organization.

The rest of the paper is structured as follows. In section 2, we present the self-organized model proposed by Levina *et al* for neuronal avalanches. A discussion of its main properties appears in sections 3 (numerical) and 4 (analytical). Then, in section 5, we put this model into the general framework of self-organized quasi-criticality introduced in [4] by deriving explicitly a Langevin equation from its microscopic rules, emphasizing the lack of true generic criticality. Finally, the main conclusions and a critical discussion of recent experimental results are presented.

2. The Levina–Herrmann–Geisel (LHG) model

Aiming at understanding the origin of power law distributed cortical avalanches, Levina, Herrmann, and Geisel (LHG) [29] proposed a variation of the well-known Markram–

J. Stat. Mech. (2010) P02015

Tsodyks model of chemical synapses [17]. Such a model had been already extensively used to reproduce the dynamics of synchronized bursting events (also called 'population spikes') [17, 32].

Consider a *fully connected network* of N **integrate-and-fire neurons** each of them characterized by its local (membrane) potential, V_i, with

$$0 \leq V_i \leq V_{\max}. \tag{2}$$

Neurons i and j (with $i \neq j$) are connected by a synapse of strength J_{ij}. This can be thought of as the amount of available neurotransmitters or, more generally, 'synaptic resources', for such a connection.

In the original Markram–Tsodyks model [17], together with V_i and J_{ij}, there is a third variable, $u_{i,j}$, representing the fraction of neurotransmitters which are actually released every time a pulse is transmitted between i and j. Its dynamics can be used to implement synaptic facilitation (see, for instance, [33]); but, aiming at keeping the model as simple as possible, and following LHG [29], we fix $u_{i,j} = u$ to be a constant.

The simplified Markram–Tsodyks or LHG dynamics is defined using the following equations:

$$\begin{aligned} \frac{\partial V_i}{\partial t} &= I^{\text{ext}}\delta(t - t^i_{\text{driv}}) + \sum_{j=1}^{N-1} \frac{uJ_{i,j}}{N-1}\delta(t - t^j_{\text{sp}}) - V_{\max}\delta(t - t^i_{\text{sp}}) \\ \frac{\partial J_{i,j}}{\partial t} &= \frac{1}{\tau_J}\left(\frac{\alpha}{u} - J_{i,j}\right) - uJ_{i,j}\delta(t - t^j_{\text{sp}}). \end{aligned} \tag{3}$$

The different terms in equation (3) are as follows:

- *Driving*: I^{ext} is the amplitude of an external random input which operates at discrete times t^i_{driv} on i. Driving impulses can be introduced at a fixed rate h. Alternatively, slow driving ($h \to \infty$) can be implemented by switching I^{ext} on if and only if all potentials are below threshold.
- *Firing*: $-V_{\max}\delta(t - t^i_{\text{sp}})$; if the potential at i overcomes the threshold, $V_{\max}$, at time t^i_{sp}, the neuron spikes, and it is reset to

$$V_i(t^i_{\text{sp}}) \to V_i(t^i_{\text{sp}}) - V_{\max}; \tag{4}$$

  otherwise, nothing happens.
- *Integration*: $\sum_{j=1}^{N-1}(uJ_{i,j}/(N-1))\delta(t - t^j_{\text{sp}})$; the (post-synaptic) neuron i integrates signals of amplitude $uJ_{i,j}/(N-1)$ from each spiking (pre-synaptic) neuron j. A non-vanishing delay between the time of discharge and the time of integration in neighboring neurons could also be introduced, without significantly affecting the results.
- *Synaptic depression*: $-uJ_{i,j}\delta(t - t^j_{\text{sp}})$; after each discharge involving the (pre-synaptic) neuron j, all synaptic strengths J_{ij} (where i runs over all post-synaptic neurons) diminish by a fraction u.
- *Synaptic recovery*: $(1/\tau_J)((\alpha/u) - J_{i,j})$; synapses recover to some target value, $J_{ij} = J = \alpha/u$, on a time scale determined by the recovery time, τ_J.

doi:10.1088/1742-5468/2010/02/P02015

J. Stat. Mech. (2010) P02015

Observe that the only sources of stochasticity are the initial condition and the external driving process, while the avalanche dynamics is purely deterministic. Also, the set of equations above can be implemented on any generic network topology; here (following LHG) we will mostly restrict our consideration to fully connected networks, although results for random networks and two-dimensional lattices are also briefly discussed.

3. Model analysis

3.1. The static limit

Let us first discuss the *static limit* of the model in which the synaptic recovery rate is so fast (i.e. $\tau_J \to 0$) that $J_{i,j}$ can be taken as a constant for all pairs i, j and for all times: $J_{i,j} = J = \alpha^{\text{static}}/u$. In such a case (keeping u fixed), α^{static} acts as a control parameter [34]. Observe that, in the limit in which $\alpha^{\text{static}} \to V_{\max}$, the model becomes conserving: each spiking neuron reduces its potential by $V_{\max}$ and each of its $(N-1)$ neighbors is increased by $V_{\max}/(N-1)$ (integration term in equation (3)).

Once the system has reached its steady state, it is possible to assume that the values of V are uniformly distributed in the interval $[\epsilon, V_{\max} - \epsilon]$ with $\epsilon \to 0$ when $N \to \infty$. This assumption parallels what is done in a similar analysis of related self-organized systems such as earthquake models [35] and can be numerically verified to hold with good accuracy (see the appendix). This implies that, fixing (without loss of generality) $V_{\max} = 1$, in the large system size limit, a randomly chosen neuron can be in any possible state with uniform probability. Thus, upon receiving a discharge of size $uJ/(N-1)$, it becomes over threshold with probability $uJ/(N-1)$. Hence, viewing the propagation of activity within avalanches as a *branching process* with branching rate $uJ/(N-1)$ and $N-1$ neighbors per neuron, the average avalanche size $\langle s \rangle$ can be written as the sum of an infinite geometric series [21]

$$\langle s \rangle = \frac{1}{1 - (N-1)\, uJ/(N-1)} = \frac{1}{1 - uJ}. \tag{5}$$

Observe that this expression is valid only for $uJ < 1$. The model critical point can be identified by the presence of a divergence in equation (5); this occurs at the conserving limit $\alpha_{\text{c}}^{\text{static}} = 1$, in agreement with what happens in other models of SOC (like sandpiles) which are critical only in the case of conserving dynamics.

For $\alpha^{\text{static}} > 1$ (i.e. above the conserving limit) the potential at each site grows unboundedly (i.e. there is no stationary state) with perennial activity (generating an 'explosive' supercritical phase) while, for $\alpha^{\text{static}} < 1$, the process is dissipative on average, i.e. the total potential is reduced at every spike and avalanches die after a characteristic time (subcritical phase). Thus, in summary, as already discussed in the literature [34], *the static version of the LHG model exhibits a standard (absorbing) phase transition separating a subcritical from a supercritical phase.*

Let us remark that, for finite systems, the critical point has size-dependent corrections. It is only in the infinite size limit, in which driving and dissipation vanish, that $\alpha_{\text{c}}^{\text{static}} = uJ_{\text{c}} = 1$. Actually, for any finite system, $\epsilon \neq 0$, and additional finite size terms need to be included in the calculation above. This is a consequence of the fact that, in order to achieve a steady state for finite systems, some form of dissipation needs to be present to compensate for the non-vanishing driving, I^{ext}, entailing $\alpha_{\text{c}}^{\text{static}}(N) < \alpha_{\text{c}}^{\text{static}}(N \to \infty) = 1$

J. Stat. Mech. (2010) P02015

Table 1. Location of the critical point α_c^{static} as a function of the system size N, as obtained in computer simulations of the *static* model ($\tau_J \to 0$). The critical point location does not depend on the way the system is driven, i.e. on I^{ext}.

N	300	500	700	1000	2000	3000	...	∞
α_c^{static}	0.92(1)	0.93(1)	0.94(1)	0.95(1)	0.96(1)	0.97(1)	...	1

(see table 1 where numerical estimates for the critical point location are reported; details of the computational procedure are reported in section 3.2).

3.2. The dynamic model

Let us now turn back to the full *dynamic* model. Observe that:

- The equation for $J_{i,j}$ in equation (3) includes a loading mechanism (analogous to those reported in [4] for earthquake and forest-fire models) or 'synaptic recovery mechanism' which counterbalances the effect of synaptic depression in the absence of spikes: the 'background field' J_{ij} increases steadily towards its target value α/u. Note that in contrast with models of forest fires or earthquake automata, in which the 'loading mechanism' (see [4]) acts only between avalanches, the recovery dynamics of J occurs also during avalanches, at a finite time scale controlled by τ_J.
- In the limit in which $u\langle J_{i,j}\rangle \to V_{\max}\ \forall(i,j)$, where $\langle\cdot\rangle$ stands for steady-state time averages, conservation is recovered *on average*. In analogy with the static model, the dynamics becomes non-stationary above such a limit: loading overcomes dissipation and potential fields grow unboundedly.

In the case in which I_{ext} drives the system slowly we are in the presence of the main ingredients characteristic of non-conserving self-organized models, as described generically in [4]:

(i) separation of (driving and dynamics) time scales,
(ii) dissipative dynamics (provided that $u\langle J_{i,j}\rangle < V_{\max}$), and
(iii) a loading mechanism, increasing the average value of the 'background field' J_{ij}.

Prior to delving into further analytical calculations, which are left for section 4, let us present in the rest of this section computational results obtained for equation (3).

3.2.1. Numerical analyses. Numerical integration of equation (3) becomes very costly as the number of components grows, limiting the maximum system size (up to $N = 3000$ in the present study). Observe that, owing to the presence of δ-functions, equation (3) is an 'impulsive dynamics' equation and thus one must proceed with caution when integrating it numerically so as not to miss delta peaks when discretizing.

The system is initialized with arbitrary (random) values of $V_i \in [0, V_{\max}]$ and $J_{i,j} \in [0,1]$, $\forall(i,j)$. We keep α as a control parameter and fix parameter values mostly as in [29]: $u = 0.2$, $V_{\max} = 1$ and $\tau_J = 10N$.

Let us remark that the choice $\tau_J = 10N$ [29] might be not very realistic from a neuroscientific point of view; i.e. it is not clear whether the synaptic recovery rate should depend

J. Stat. Mech. (2010) P02015

on the total number of connections of the corresponding neuron or not. Observe that N is the number of synapses per neuron; therefore in principle, it could be the case that, if a given neuron has limited resources, the recovery rate per synapse depends on the total number of synapses. But also the opposite could be true; i.e. the recovery time of a given synapse could depend only on its local properties and not on those of its corresponding neuron. This is a neuro-scientific issue that is beyond the scope of the present paper and that we prefer not to address here. Anyway, we have verified that our results are not significantly affected by such a choice; for example, we have also considered values of τ fixed for any N and checked the robustness of our results.

We work in the slow driving limit, i.e. we drive the system with an input, $I_{\rm ext}$, at a randomly chosen site if and only if all potentials are below threshold. The sequence of activity generated therefrom constitutes an avalanche. We have used two different dependences on N for $I^{\rm ext}$: (i) $I^{\rm ext} = 7.5 \times N^{-1}$ and (ii) $I^{\rm ext} = N^{-0.6467}$, both of them engineered to comply with the scaling form $I^{\rm ext} \sim N^{-w}$ considered by Levina *et al*, and to reproduce the value $I^{\rm ext} = 0.025$ for $N = 300$ used in simulations in [29]. Results are mostly insensitive to the choice of $I^{\rm ext}$.

Running computer simulations of equation (3) with this set of parameters, a steady state for both V_i and $J_{i,j}$ is eventually reached, after an initial transient. In such a regime, driving events generate avalanches of activity. Figure 1 shows time series in the steady state for the network-averaged value of $uJ_{i,j}$, $u\bar{J}$, with

$$\bar{J}(t) \equiv \sum_{i,j,\ i\neq j} \frac{J_{i,j}(t)}{N(N-1)}. \tag{6}$$

Results correspond to $N = 1000$ and three different values of α, 0.9, 1.4 and 1.9. Large avalanches (which are much more frequent in the supercritical phases) correspond to abrupt falls in $u\bar{J}$, while in between avalanches $u\bar{J}$ grows linearly in time owing to the external driving.

Observe the intermittent response of the system in all cases: peaks of activity of various sizes appear in all cases; note also the 'quasi-periodic' behavior in all the three cases (similar quasi-periodic behavior had already been described for the Markram–Tsodyks model [32, 36]).

In order to determine the critical point, in figure 2 (left) we show the associated avalanche size distributions for the same three values of α. All of them show for small values of s a power law decay, with exponent close to 1.5; for $\alpha = 0.9$ (subcritical) there is an exponential cut-off while for $\alpha = 1.9$ (supercritical) there is a 'bump' for large size values, which defines a characteristic scale. In the intermediate case, $\alpha = 1.4$, there is also an exponential cut-off but, with increasing system size, it shifts progressively to the right in a scale-invariant way, corresponding to a critical point. This is illustrated in figure 2 (right) where critical distributions (i.e. for $\alpha = 1.4$) for various system sizes have been collapsed into a unique scale-invariant curve.

In figure 3 (top) we plot the distributions of $u\bar{J}$ for different values of α, obtained by sampling values of $\bar{J}$ throughout the dynamics. Observe the progressive broadening and displacement to the right upon increasing α.

Figure 3 (bottom) illustrates the presence of strong finite size effects; in particular, for the critical point $\alpha = 1.4$, we see that the distribution of $\bar{J}$ moves progressively to the right. The main observation to be made is that these distributions *do not* converge to

doi:10.1088/1742-5468/2010/02/P02015

J. Stat. Mech. (2010) P02015

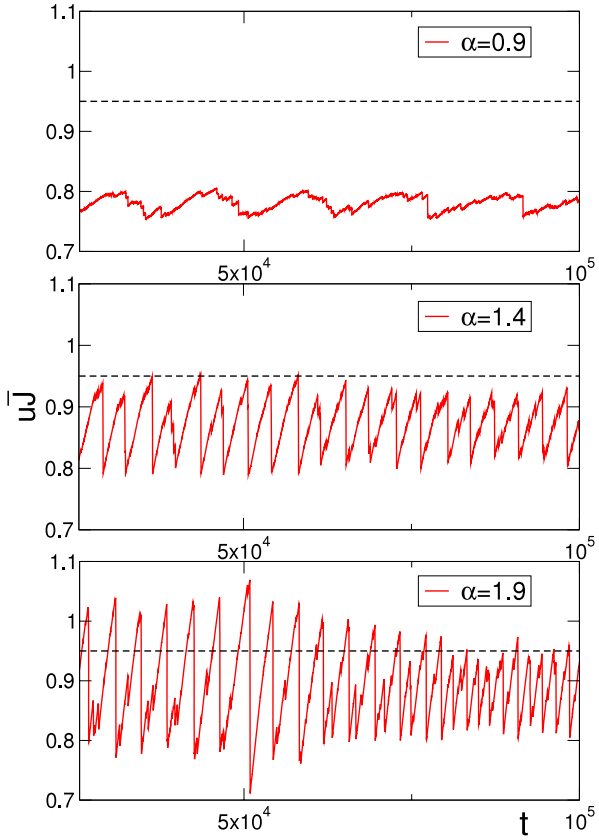

Figure 1. Time evolution of $u\bar{J}$ and the number of spiking neurons for $\alpha = 0.9$, subcritical (up), $\alpha = 1.4$, critical (center), and $\alpha = 1.9$, supercritical (down), in simulations with $N = 1000$. It is only above the critical point of the dynamical model that $u\bar{J}$ goes beyond the critical point of the static model for the system size considered, $\alpha_c^{\text{static}} = 0.95(1)$ (dashed line).

narrower ones upon enlarging the system size. Similar broad distributions are typical of non-conserving self-organized models, for which delta-peaked distributions are *not* obtained even if the infinite size limit is taken [4]. This means that the dynamical model does not correspond to the static one with some fixed 'effective' or averaged value of $\bar{J}$, but to a *dynamical convolution* of different values of $\bar{J}$, distributed in some interval $[\bar{J}_{\min}(\alpha), \bar{J}_{\max}(\alpha)]$, with weights given by the distributions above. The probability of finding the system at any point out of such an interval $[\bar{J}_{\min}(\alpha), \bar{J}_{\max}(\alpha)]$ is zero (within numerical precision).

As illustrated in figure 4 we have verified that for $u\langle\bar{J}\rangle > 1$ (which occurs for large values of α; in particular, for $\alpha \to \infty$ in the $N \to \infty$ limit), the loading mechanism dominates over the discharging one (synaptic depression), and the potential grows unboundedly with never ceasing activity; this is a non-stationary supercritical or *explosive phase*, analogous to the one reported for the static version of the model.

Finally, we have also computed the average value of J *at spike*, i.e. right before the corresponding pre-synaptic neuron fires and before the value of J is diminished (see figure 5). This quantity, that we call J_{sp}, appears in the analytical approach to be discussed

J. Stat. Mech. (2010) P02015

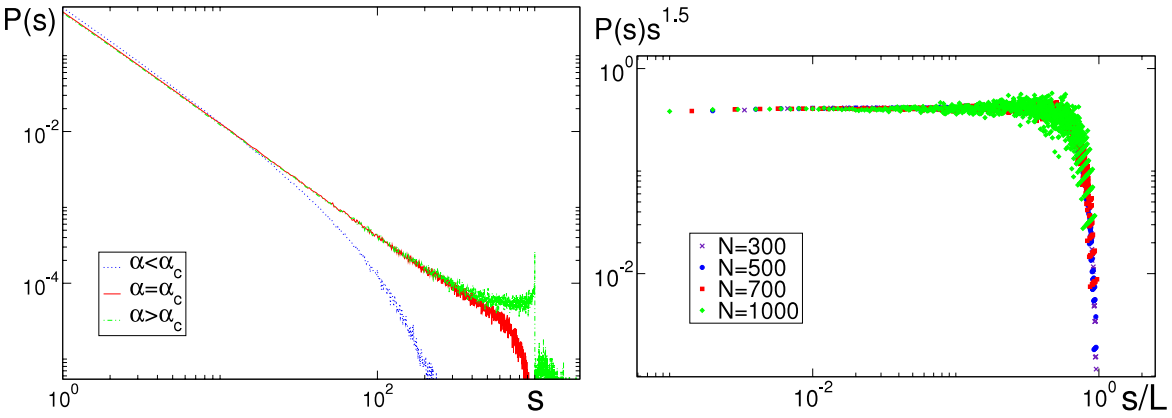

Figure 2. Left: avalanche size distribution of the LHG model for $N = 1000$ and three different values of α, 0.9, 1.4 and 1.9 (slightly below, at, and slightly above the critical point, respectively). Right: rescaled avalanche size distribution showing good finite size scaling. This implies that the cut-off for the critical value (see left) shifts progressively to the right, in a scale-invariant way, upon enlarging the system size.

below. Observe in figure 5, in analogy with the histograms above, the existence of broad distributions whose width does not decrease significantly upon enlarging the system size. Analyzing the highly non-trivial structure of these (multi-peaked) histograms is beyond the scope of this paper, but let us just mention that similar histograms with various peaks appear in the related non-conserving model of SOqC [35]. Note also that they extend beyond $uJ_{\rm sp} = 1$, even if their average is close to unity.

3.2.2. Characterization of criticality. Perusal of either figure 1 or figure 3 (top) leads to the important observation that it is only for values of α above the critical point ($\alpha_{\rm c} \approx 1.4$) that the support of the distribution of $u\bar{J}$ extends beyond the (N-dependent) critical point of the static limit, i.e. that $u\bar{J}_{\rm max} \geq \alpha_{\rm c}^{\rm static}(N)$ (see figure 3 (upper)). For $\alpha < \alpha_{\rm c}$ the dynamics is subcritical at every time (i.e. $u\bar{J}_{\rm max}(N)$ is always below the threshold of the static model, $\alpha_{\rm c}^{\rm static}(N)$), and hence avalanche distributions, being a dynamical convolution of avalanches with instantaneous subcritical parameters, are subcritical. Instead for $\alpha > \alpha_{\rm c}$, $u\bar{J}_{\rm max} > \alpha_{\rm c}^{\rm static}(N)$, and one can observe instantaneous values of the average synaptic strength, $\bar{J}$, above the static model critical point, giving rise to instantaneous supercritical dynamics and system-wide propagation (observe that, in a fully connected topology, any site/neuron can be reached within one time step). Then, during the avalanche, owing to the term $-uJ_{ij}\delta(t - t_{\rm sp}^j)$ in the second equation of equation (3), $u\bar{J}$ decreases, and the system moves progressively from the supercritical regime to the subcritical one. This, in turn, becomes supercritical again upon recovering/loading. This cyclical shifting (analogous to that for SOqC as described in [4]) provides a dynamical mechanism for the generation of a broad distribution of avalanche sizes in the steady state.

Thus, it is only for $\alpha > \alpha_{\rm c}$ that arbitrarily large avalanches appear, and *the critical point of the dynamical model corresponds, for any system size, to the value of* α *for which the maximum of the support of the distribution of values of* $\bar{J}$, $\bar{J}_{\rm max}$, *coincides with the*

J. Stat. Mech. (2010) P02015

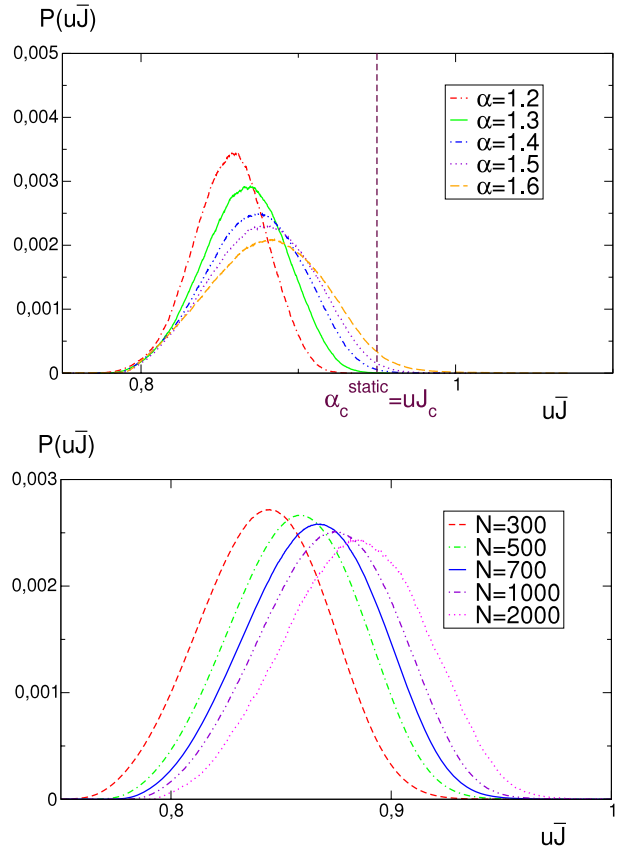

Figure 3. Top: Probability distribution of $u\bar{J}$ for a system size $N = 1000$ and different values of α. Only for $\alpha > \alpha_c = 1.4(1)$ does the right tail of the distribution extend beyond the critical value of the static model $\alpha_c^{\rm static}(N = 1000) = uJ_c = 0.95$. Bottom: $P(u\bar{J})$ at the critical point, $\alpha_c = 1.4$, for different system sizes; the width of the distribution does *not* decay with increasing system size and, therefore, this distribution is *not* delta-peaked in the thermodynamic limit. This reflects the fact that, for sufficiently large values of α the system hovers around the critical point, alternating subcritical and supercritical regimes. For smaller values of α the system is always subcritical.

critical point of the static model:

$$u\bar{J}_{\rm max} = \alpha_c^{\rm static} = uJ_c. \tag{7}$$

Figure 6 (left) illustrates the coincidence (within numerical resolution) of the critical line for the static model, $uJ_c(N)$, and the maximum of the support of the distribution of $\bar{J}$ at the critical point of the dynamical model for various system sizes. The small deviation between the two curves stems from the binning procedure employed to determine $\bar{J}_{\rm max}$.

The average value of $\bar{J}$ at the critical point is also plotted in figure 6 (left) for illustration: at criticality, the average value is always far below unity, i.e. far below the conserving limit. Even in the infinite size limit, this curve remains below 1 (as a consequence of the fact that the maximum of the distribution converges to 1 and the distribution is not a delta function).

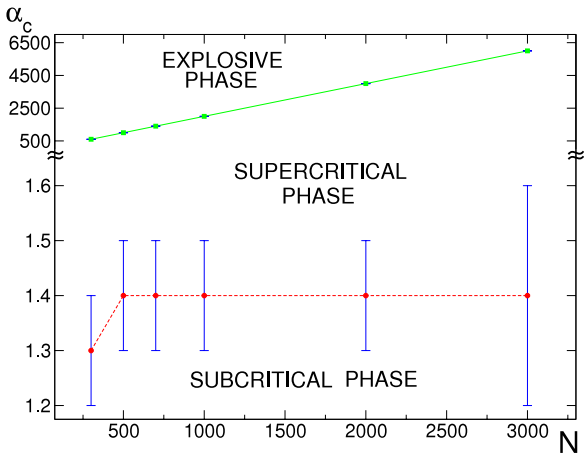

Figure 4. Phase diagram for the LHG model for different system sizes. Observe the presence of a critical line separating an active (supercritical) from an absorbing (subcritical) phase. Also, for large values of α a non-stationary or 'explosive' phase (in which potentials grow unboundedly) exists.

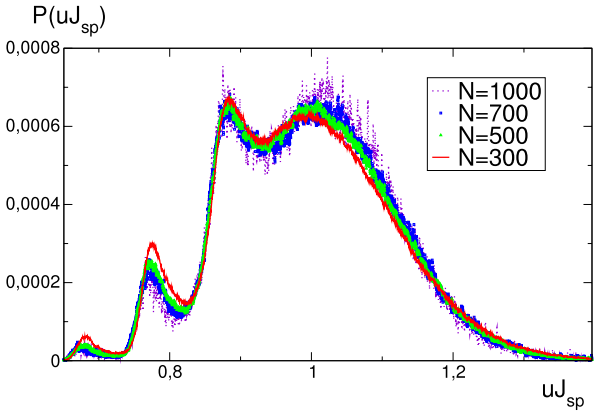

Figure 5. Probability distribution of values of uJ computed *at spike*, i.e. at their local maxima, just before being depressed. Curves correspond to different system sizes (from 300 to 1000) and fixed α, $\alpha = 4 > \alpha_c$, i.e. in the supercritical phase. Observe the broad distribution, whose width does not decrease significantly upon enlarging the system size. Similar broad histograms, typical of SOqC systems, are obtained for other values of α.

Using our numerical estimates of the critical point as a function of N (taken from figure 6 (left)) we have shown (see figure 6 (right)) that the critical point converges to unity as $1 - u\bar{J}_{\max}(N) \sim N^{-0.36(6)}$. The same property holds for the static model, for which we obtain $1 - uJ_c(N)) \sim N^{-0.36(6)}$. This illustrates that the progressive shifting of the distributions in figure 3 (bottom) to the right occurs at the same pace as that of the critical point of the static model, in such a way that our estimate of the critical point, α_c, is hardly sensitive to finite size effects: for every system size studied, we obtain $\alpha_c(N) \approx 1.4(1)$ as illustrated in figure 4.

Using the absorbing state picture of non-conserving self-organized systems, which predicts scaling to be controlled by a *dynamical percolation* critical point, we made the

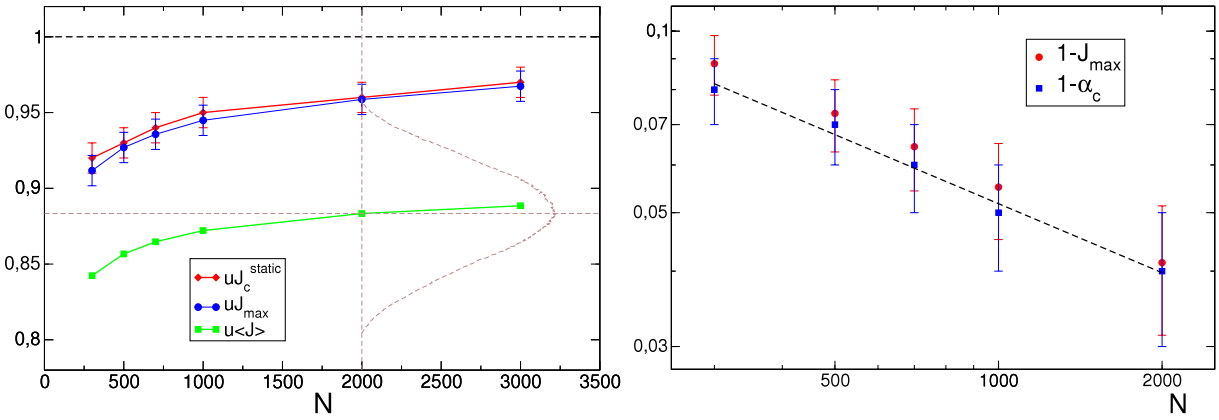

Figure 6. Left: critical value of J, J_c, in the static model (upper curve), maximum of the support of the distribution of $\bar{J}$, $J_{\max}$, in the dynamic model (central curve), and average value of $\bar{J}$, i.e. $\langle \bar{J} \rangle$, at the critical point (lower curve). Note that this last curve lies in the subcritical region: $\langle \bar{J} \rangle$ is not equal to 1 at the critical point. The dashed bell-shaped curve represents in a sketchy way the $\bar{J}$ probability distribution for $N = 2000$; its height is unrelated to the x-coordinate in the main graph; the peak is located around 0.88 (in coincidence with the $\langle \bar{J} \rangle$ curve), while the upper tail of the distribution 'touches' the vertical line, around 0.95 (i.e. at the corresponding point in the $J_{\max}$ curve). Right: scaling of the distance to the infinite size critical point (i.e. 1) in both the static and the dynamic LHG models as a function of the system size. As predicted by the general theory for non-conserving self-organized models, they both are power laws with an exponent close to 1/3 (dashed line).

quantitative prediction that, for generic SOqC systems, the finite size correction to the critical point should scale with system size as $N^{-1/3}$ (see [4] and section 5 below). In our case,

$$u\bar{J}_{\max}(N \to \infty) - u\bar{J}_{\max}(N) \sim N^{-1/3}, \tag{8}$$

in agreement with the numerical estimates (see the dashed line in figure 6 (right)). This supports the validity of the theoretical framework presented in [4] to account for the present model: the critical behavior of neural avalanches is controlled by a *dynamical percolation* critical point.

Before finishing this section, let us briefly present some results for the LHG model implemented on different kinds of topologies. In particular, we have numerically studied a version with a finite connectivity (random neighbors) as well as a two-dimensional lattice. In both cases, we find subcritical and supercritical phases separated by a critical point, as in the fully connected lattice.

For the random neighbor case, some details, such as the way the cut-offs scale with system size, are different, but the main results are as in the fully connected case.

For the two-dimensional lattice, figure 7 illustrates the evolution of an avalanche of activity for a particular value of α (in the supercritical regime). Observe the presence of a noisy wave of activity propagating outward from the seed; similar avalanches cannot be visualized in the fully connected case where activity reaches all sites in a single time step.

J. Stat. Mech. (2010) P02015

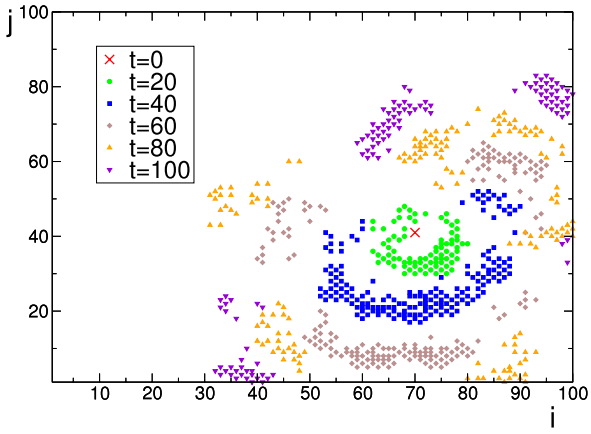

Figure 7. Propagation of activity as a function of time in a two-dimensional (100×100) implementation of the LHG model, for $\alpha = 2$, in the supercritical phase.

The waves shown in figure 7 resemble very much the ones observed in the retina (which is an almost two-dimensional network) before maturation [37] and, more importantly for the discussion here: they are fully analogous to supercritical waves appearing in

- other non-conserving self-organized systems such as forest fires and
- the dynamical percolation theory in the supercritical regime.

This observation confirms, once again, the very close relationship between the LHG model and the theory of SOqC [4].

In summary, the LHG model is a representative of the class of non-conserving self-organized systems or SOqC, which, as shown in a previous paper [4], exhibits a conventional critical point separating a subcritical from a supercritical phase. Criticality is controlled by the maximum of the support distribution of $\bar{J}$, $\bar{J}_{\max}$, and not by its average value. This is in accordance with the general criterion for criticality in SOqC systems put forward in [4]: criticality emerges when the temporarily changing background field, $\bar{J}$, overlaps with the active phase of the underlying (static) absorbing state phase transition [4]. This result is of relevance for the analytical approach in the next section

4. Analytical results

The main conclusion of the previous section, i.e. the need to fine-tune α to observe true criticality, seems to be in disagreement with the one presented in [29] for the LHG model. There it was claimed, relying on a mean-field calculation, that all values of α in the interval $[1, \infty[$ are strictly critical. Using the hindsight gained from the results above, it is not difficult to find where the problem lies, as we show in what follows.

Let us first construct (following LHG) a balance equation for the static limit of the model. Calling the inter-spike interval Δ^{isi} (the time between two consecutive spikes of *a given neuron*) and the inter-avalanche interval Δ^{iai} (the time between two consecutive avalanches, starting at *any neuron*), the average number of avalanches between two spikes

J. Stat. Mech. (2010) P02015

of the same neuron, $\langle M \rangle$, is

$$\langle M \rangle = \frac{\Delta^{\text{isi}}}{\Delta^{\text{iai}}}. \tag{9}$$

Obviously, Δ^{iai} has to be inversely proportional to I^{ext}: if the external driving is reduced by a factor r the average time for generating an avalanche grows by a factor r. Levina *et al* [29] actually showed that

$$\Delta^{\text{iai}} = \frac{V_{\text{max}} - \epsilon(N)}{I^{\text{ext}}}, \tag{10}$$

where, as above, $\epsilon(N)$ vanishes for $N \to \infty$. Focusing on a single neuron, in the steady state, it must obey the following balance equation:

$$V_{\text{max}} = \frac{I^{\text{ext}}}{N}\Delta^{\text{isi}} + \frac{uJ}{N-1}\langle s \rangle \langle M \rangle, \tag{11}$$

which equates the potential decrease for each spike (lhs term) to the total potential increase between two consecutive spikes; this comes from two possible sources: (1) the average loading owing to external driving between two consecutive spikes (first term in the rhs) and (2) the average charging from avalanches (second term). Note that $N-1$ is the number of neighbors of a given neuron and $\langle s \rangle$ is the averaged avalanche size. Fixing $V_{\text{max}} = 1$, $\epsilon(N) = 0$, and plugging equations (9) and (10) into (11), one readily obtains

$$\frac{N}{\Delta^{\text{isi}} I^{\text{ext}}} \propto uJ\langle s \rangle \tag{12}$$

for large values of N.

In the *static case*, $\langle s \rangle$ is given by equation (5), so Δ^{isi} can be expressed as a function of J, N and I^{ext}. We have numerically verified that the resulting balance equation holds.

On the other hand, in the *dynamical case*, J is not a constant and we do not have a simple expression for $\langle s \rangle$. The authors of [29] assume that the average avalanche size can still be written using equation (5) but replacing uJ by $u\langle J_{\text{sp}} \rangle$. In particular, it is hypothesized that avalanches can be effectively described as static avalanches with an effective branching rate given by the average branching ratio *at spike* (i.e. the synapses which are about to spike are the ones controlling the branching process of activity); this is

$$\langle s \rangle = \frac{1}{1 - u\langle J_{\text{sp}} \rangle}. \tag{13}$$

This equality is expected to hold in the infinite system size limit and for infinitely large avalanches (where the law of large numbers applies) in which case the average of sampled values of J_{sp} during sufficiently large avalanches can be safely replaced by $\langle J_{\text{sp}} \rangle$. In any case, it can be valid only for branching ratios up to 1 (for which the geometric series converges). Substituting equations (13) into (12) LHG we readily obtain

$$u\langle J_{\text{sp}} \rangle = \frac{N^2 - \Delta^{\text{isi}} I^{\text{ext}} N}{N^2 + \Delta^{\text{isi}} I^{\text{ext}}} \tag{14}$$

which, trivially, is smaller than or, at most, equal to 1. From this, one concludes that the effective branching process is either subcritical or critical, but cannot be supercritical. Two comments are in order:

J. Stat. Mech. (2010) P02015

The first one is that equation (12) is valid if and only if $u\langle J_{\rm sp}\rangle$ is not larger than 1; hence, the calculation above does not exclude the possibility of the existence of other (supercritical) solutions, for which equation (12) would not hold. Actually, as illustrated in the numerics, for any finite system, an exploding phase, with branching ratio larger than unity, does exist (as a mater of fact, given a fixed value of α, depending on how the 'loading' constant τ_J is scaled with system size, i.e. depending on how fast the recovery of synapses is, one can shift the location of the critical point and enlarge or reduce the size of the supercritical region).

The second one is as follows: the main approximation of the calculation above is the replacement of the average of sampled values of $J_{\rm sp}$ during any sufficiently large avalanche by $\langle J_{\rm sp}\rangle$. If, during avalanche propagation, the uncovering of values of $J_{\rm sp}$ from $P(J_{\rm sp})$ (which is depicted in figure 5 for a particular value of α) occurred in a random, *uncorrelated*, way then the process would be what is called in the literature a 'branching process in a random environment' [38]. Such a process turns out to be controlled by the average value of the random branching ratio [38]. In such a case, the calculation would be exact and, for any value of α for which the average branching ratio is unity, the process would be critical.

However, the uncovering of values of $J_{\rm sp}$ in the LHG model exhibits *strong correlations*. $J_{\rm sp}$ fluctuates around the central value $uJ_{\rm sp} = 1$ in a rather correlated way. This is illustrated in figure 8, where we plot a return map for of $uJ_{\rm sp}$ averaged throughout each single avalanche. Notice that the return map is not structureless as would correspond to a random process. Instead, the system is progressively charged towards large values of the synaptic intensity and, afterward, it gets suddenly discharged, starting a new cycle. In this way, the true dynamics of the system consists of a continuous alternation of supercritical (where most of the $J_{\rm sp}$ take values above 1) and subcritical dynamics: individual avalanches are either subcritical (average branching ratio smaller than 1) or supercritical (average branching ratio above 1), and hence the resulting avalanche size distribution is a complex one (not a simple power law). This is illustrated in figure 9 which shows the avalanche size distribution for different system sizes and $\alpha = 4$ in the supercritical phase (the rest of parameters are as in figure 5). Although the averages of $uJ_{\rm sp}$ (as calculated from figure 5) are very close to 1 for all sizes, the curves in figure 5 show a bump at large avalanche sizes, reflecting the presence of many supercritical avalanches. This effect does not decrease upon increasing system size, although the bump moves progressively to larger values as the system size is increased. Similarly, correlations are also responsible for the shift from the predicted mean-field critical point $\alpha = 1$ to the actual one $\alpha_{\rm c} \approx 1.4$.

In conclusion: although the branching ratio turns out to be always very close to unity for any value of $\alpha \geq \alpha_{\rm c}$, the avalanche size distributions are not generically pure power laws. In the supercritical phase there are bumps revealing a not truly scale-invariant nature. This conclusion is in agreement with the general scenario for non-conserving self-organized systems introduced in [4].

As a final remark, we want to emphasize that the results by Levina *et al* are mostly correct: the branching ratio is actually equal to unity in a broad region of parameter space (in the infinitely large system size limit). However, as explained above, this 'marginality' of the averaged branching ratio does not exactly correspond generically to true scale invariance.

J. Stat. Mech. (2010) P02015

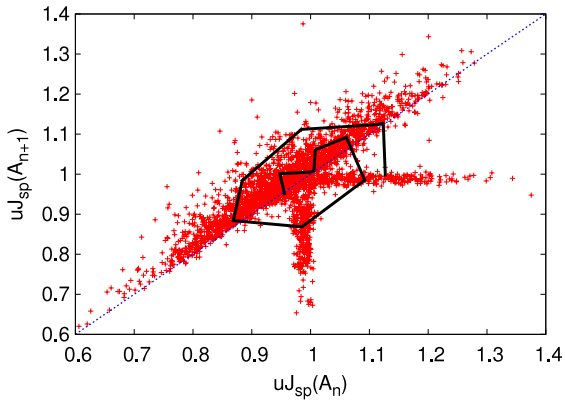

Figure 8. Return map for $uJ_{\rm sp}$ averaged over two consecutive avalanches A_n and A_{n+1} in the supercritical regime. The broken line joins (clockwise) 20 consecutive points of the map to illustrate the temporal structure of the charging–discharging cycle. The non-trivial structure of the map reflects the presence of strong correlations: the system typically moves up in a few steps along the main diagonal (see the broken line) and then, after reaching the supercritical regime $uJ_{\rm sp} > 1$, a large avalanche is produced, and the system returns to the subcritical regime $uJ_{\rm sp} < 1$, to start a new charging–discharging cycle. The diagonal dashed line, $uJ_{\rm sp}(A_{n+1}) = uJ_{\rm sp}(A_n)$, is plotted as a guide to the eye.

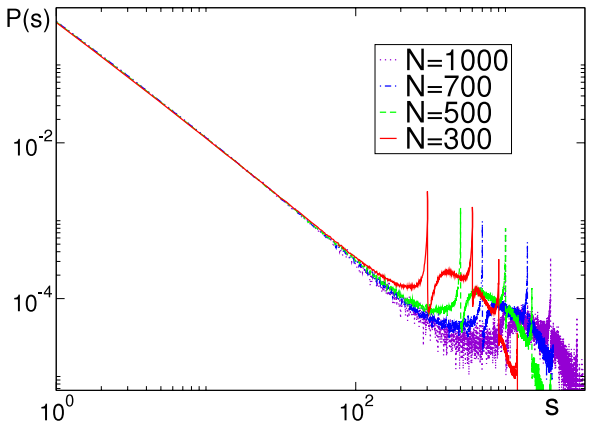

Figure 9. Avalanche size distribution for $\alpha = 4$ (the rest of the parameters are as in the plots above) and different system sizes (as in figure 5) Observe the presence of bumps, which do not disappear on increasing the system size. This illustrates the existence of a supercritical phase in the LHG model.

The main virtue of the LHG model is that, although not generically critical, it generates a rather broad 'pseudo-critical' region, exhibiting partial power laws. The ultimate reason for this is rooted in the extremely slow loading (recovering) process of the background field (synaptic strength), which occurs during avalanches. This is to be compared with the more abrupt loading in forest-fire and earthquake models, which occurs between avalanches. This more abrupt loading induces excursions around the critical point to be broader than their counterparts in the LHG model. This is particularly true in the (probably unrealistic) case in which τ_J diverges with the system size.

J. Stat. Mech. (2010) P02015

5. A simple absorbing state Langevin equation approach

In order to obtain a more explicit connection between the LHG model and the family of SOqC models and theory discussed in [4], in this section we construct a Langevin equation for the LHG model, which includes absorbing states (and is therefore a natural extension of the Langevin theory for SOC, as introduced in [2, 39, 40]) and turns out to be almost identical to the general Langevin theory for SOqC systems (as introduced in [4]).

For the sake of simplicity, and without loss of generality, let us consider homogeneous initial conditions for all V_i and $J_{i,j}$, i.e. $V_i = V\ \forall i$ and $J_{i,j} = J\ \forall i, j$, and also, $I^{\text{ext}} = 0$. Under these conditions, and given the deterministic character of the dynamics, all neurons evolve synchronously and equations (3) can be simply rewritten as

$$\begin{aligned} \partial_t V &= [uJ - V_{\max}]\,\delta(t - t_{\text{sp}}) \\ \partial_t J &= \frac{1}{\tau_J}\left(\frac{\alpha}{u} - J\right) - uJ\delta(t - t_{\text{sp}}). \end{aligned} \tag{15}$$

where t_{sp} are the firing times. Let us remark that in order to treat the more general heterogeneous case it suffices to keep sub-indexes in the different variables.

The spike terms, proportional to $\delta(t - t_{\text{sp}})$, can be alternatively written as

$$\delta(t - t_{\text{sp}}) \to \rho \equiv \Theta(V - V_{\max}), \tag{16}$$

where $\Theta(x)$ is the Heaviside step function (we adopt the convention that $\Theta(0) = 0$); i.e. spike terms operate only whenever the potential is above threshold, implying that the *activity variable*, ρ, is non-zero only in such a case. Thus,

$$\begin{aligned} \partial_t V &= [uJ - V_{\max}]\,\rho \\ \partial_t J &= \frac{1}{\tau_J}\left(\frac{\alpha_J}{u} - J\right) - uJ\rho. \end{aligned} \tag{17}$$

Further analytical progress can be achieved by regularizing the step function in equation (16) as a hyperbolic tangent:

$$\rho \approx \tfrac{1}{2}\left(1 + \tanh\left[\beta\left(V - V_{\max}\right)\right]\right), \tag{18}$$

which is a good approximation provided that $\beta \gg 1$. Inverting equation (18) we obtain

$$V = \frac{\operatorname{arctanh}\left(2\rho - 1\right) + V_{\max}}{\beta} \tag{19}$$

and, taking derivatives on both sides,

$$\partial_t V = \frac{1}{2\beta}\frac{\partial_t \rho}{\rho\left(1 - \rho\right)}, \tag{20}$$

which is well defined provided $\rho \in]0, 1[$. Let us underline that the forthcoming equations are also valid at $\rho = 0$, where activity ceases. Using this, equation (17) can be rewritten as

$$\begin{aligned} \partial_t \rho &= 2\beta\left(uJ - V_{\max}\right)\rho^2\left(1 - \rho\right) \\ \partial_t J &= \frac{1}{\tau_J}\left(\frac{\alpha_J}{u} - J\right) - uJ\rho \end{aligned} \tag{21}$$

which, omitting higher order terms, reduces to

$$\begin{aligned}\partial_t \rho &= 2\beta u J \rho^2 - 2\beta V_{\max} \rho^2 \\ \partial_t J &= \frac{1}{\tau_J}\left(\frac{\alpha_J}{u} - J\right) - uJ\rho.\end{aligned} \tag{22}$$

Renaming variables as follows: $2\beta V_{\max} \to b$, $2\beta u \to w$, $J \to \phi$, $1/\tau_J \to \gamma$, $\alpha_J/u \to \phi_c$, and $u \to w_2$, one obtains

$$\begin{aligned}\partial_t \rho &= w\phi\rho^2 - b\rho^2 \\ \partial_t \phi &= \gamma\,(\phi_c - \phi) - w_2\phi\rho.\end{aligned} \tag{23}$$

The equation for ρ is a typical mean-field equation for a system with absorbing states (i.e. all dynamics ceases when $\rho = 0$). It includes a coupling term with the background field ϕ: the larger the background, the greater the degree of activity created. In the simplest possible theory of SOqC (see [4]), such a coupling is linear in ρ, but the effects of the two types of coupling can be argued to be qualitatively identical. On the other hand, the second equation is identical to the mean-field background equation for SOqC systems: the presence of activity reduces the background field while the loading mechanism, acting independently of activity, increases it.

Except for the coupling term which is quadratic in ρ, these mean-field equations are identical to the ones proposed in [4] for describing non-conserving self-organized models at a mean-field level. Also, in analogy with SOqC systems, when slow driving is switched on, i.e. $I^{\text{ext}} \neq 0$, activity can be spontaneously created, even if $\rho = 0$, generating avalanches of activity. Moreover, if some sort of stochasticity (and hence heterogeneity) is introduced into the dynamics, then it can be easily seen that:

- a noise term, proportional to $\sqrt{\rho}$, needs to be added to the first equation,
- a diffusion term accounts for the coupling with nearest neighbors, and
- a linear coupling term is perturbatively generated in the activity equation (and, thus, the quadratic coupling becomes a higher order term).

Therefore, after including fluctuations and omitting higher order terms, the final set of stochastic equations that we have derived is identical to that of *dynamical percolation* [41] in the presence of a 'loading mechanism', i.e. to that of SOqC systems as described in [4].

This heuristic mapping between the LHG model and the general theory of SOqC explains from an analytical viewpoint all the findings in previous sections (including the quantitative prediction for the finite size scaling of $(1 - uJ_{\max}(N))$) and firmly places the LHG model in the class of self-organized quasi-critical models, lacking true generic scale invariance.

6. Conclusions

Cortical avalanches, first observed by Beggs and Plenz [5], were claimed to be generically power law distributed and, thus, critical. Such a claim led to a burst of activity in neuroscience aiming at achieving an understanding of the origin and consequences of such a generic scale invariance. At a theoretical level, Levina, Herrmann, and Geisel [29] proposed a simple model (a variation of the Markram–Tsodyks model for chemical

J. Stat. Mech. (2010) P02015

synapses), claimed to reproduce scale invariance generically. In particular, these authors performed a mean-field calculation leading to the conclusion that, for any value of the control parameter, α, larger than unity, generic critical behavior is observed. They also conducted some computational studies in order to support their findings.

The LHG model turns out to be very similar to slowly driven models of self-organized criticality such as earthquake and forest-fire models. As in these other models, and in contrast to the sandpiles case, in the LHG one the dynamics is *non-conserving* (reflecting the leaking/dissipative dynamics of actual synaptic signal transmission).

It is now a well-established fact that non-conserving self-organized models are not generically critical but just 'hover around' the critical point of an underlying absorbing phase transition, with finite excursions (of tunable amplitude) into the active and the absorbing phases. As they do not converge to the critical point itself, generic scale invariance cannot be invoked (see [4] and references therein). The term self-organized quasi-criticality (SOqC) has been proposed to refer to such a class of systems, emphasizing the differences from conserving SOC models.

Given the contradiction between this general result and the claim in [29], in this paper we have scrutinized the LHG model, both numerically and analytically, and reached the following conclusions:

- Both in its static and its dynamical form, the model exhibits absorbing and active phases and a non-trivial critical point separating them.
- It is only if parameters are fine-tuned to such a critical point that true scale invariance emerges and the distribution of avalanche sizes is power law distributed.
- The mean-field calculation in [29], supporting generic criticality, did indeed lead to a branching ratio equal to unity in a broad interval of phase space, but this does not imply generic scale invariance.
- A Langevin equation, including absorbing states, has been derived for the LHG model. Such an equation reduces to the analogous one proposed for describing generically non-conserving self-organized (SOqC) models. Thus, all the general conclusions obtained from such a theory in [4] apply to the LHG model, providing analytical support to the numerical findings above.

It is worth stressing that our results do not devalue the LHG model. Actually, strict criticality might not be required to explain the truncated power laws reported by Beggs and Plenz; the dynamical LHG model generates partial power laws compatible with the empirical findings of Beggs and Plenz for a relatively broad parameter (α) interval, as shown in figure 10.

Moreover, the fact that the model can generate critical, subcritical, and supercritical regimes, depending on parameter values, converts the LHG model into one adequate for describing the *state of the art for neuronal avalanches*. As mentioned in the introduction, Pasquale *et al* have shown in a recent paper [28] that, depending on several experimental features, cortical avalanches can indeed be critical, subcritical, or supercritical.

The main implication of our work can be summarized as follows: if future experimental research conducted on cortical networks were to support critical avalanches being the norm and not the exception, then, one should look for more elaborate theories, beyond simple self-organization, to explain this. Standard self-organization does not suffice to

J. Stat. Mech. (2010) P02015

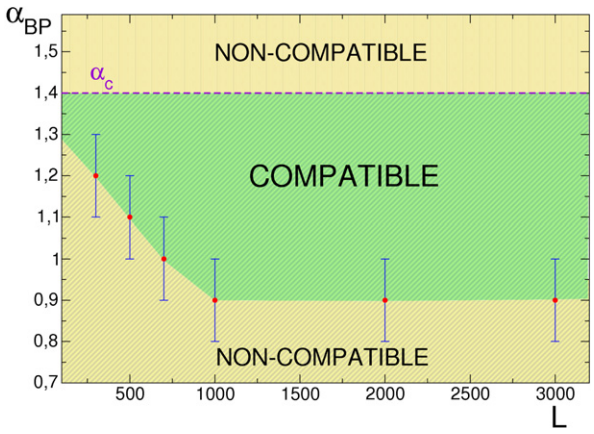

Figure 10. Range of compatibility of the results from the LHG model, for different values of N, and the empirical results of Beggs and Plenz; for large system sizes ($N > 700$) values of α between 1 and 1.4 give avalanche size distributions compatible with those observed by Beggs and Plenz [5], even if they are subcritical.

explain criticality in non-conserving systems. Parameters have to be tuned or 'selected' to achieve a close-to-criticality regime. For instance, the claim by Royer and Paré [31] that homeostatic regulation mechanisms maintain cortical neural networks with an approximately constant (i.e. *conserved*) global synaptic strength could be the basis for such a less generic theory beyond simple self-organization. Another inspiring possibility is that natural selection by means of evolutionary and adaptive processes leads to parameter selection, favoring critical or close-to-critical propagation of information in the cortex [30]. A more realistic approach should also include long-term plasticity [42], as well as co-evolutionary mechanisms, shaping the network topology. We shall explore these possibilities in a future work.

Acknowledgments

We acknowledge financial support from the Spanish MICINN-FEDER Ref. FIS2009-08451 and from Junta de Andalucía FQM-165. Useful discussions and/or e-mail exchanges with M Hennig, G Bianconi, P L Garrido, V Torre, H Chatè, I Dornic, S Johnson, and J M Beggs are gratefully acknowledged. We thank especially J Cortés and A Levina for a critical reading of the first version of the manuscript and for insightful comments.

Appendix: Synchronization and oscillatory properties

Synchronization was studied in the self-organized criticality literature as a possible mechanism, alternative to conserving dynamics, leading to generic scale invariance [43]. Even though such a suggestion turned out not to be correct [4], let us explore here the oscillatory and synchronization properties observed in numerical simulations of the LHG model. With this aim, we compute the power spectra, $S(f)$, for the time series of J shown in figure 1 (as well as for other values of α). In all cases, as illustrated in figure A.1, the spectra exhibit peaks at some characteristic frequencies, f.

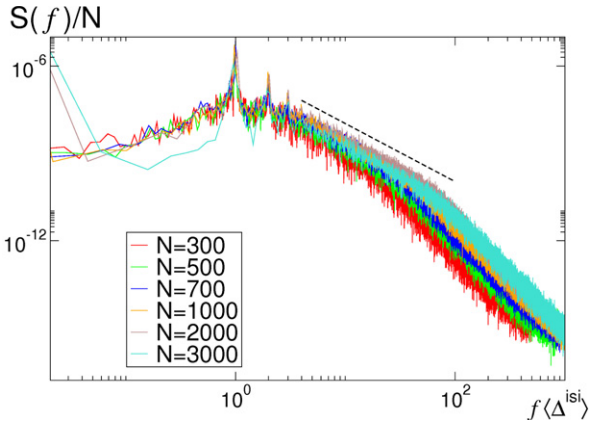

Figure A.1. Power spectrum of the LHG model for $\alpha = 2$ (i.e. supercritical). Frequencies f are plotted rescaled by a factor $\langle\Delta^{\rm isi}\rangle$. Note the presence of peaks, at $f \propto \langle\Delta^{\rm isi}\rangle^{-1}$, coexisting with fat tails. The tail decay k^{-2} (dashed line) is characteristic of sawtooth profiles (i.e. with linear increases).

Closer inspection reveals that the maximum peak appears at a characteristic frequency, $f_{\rm c}$, which we have verified to be inversely proportional to $\langle\Delta^{\rm isi}\rangle$. This indicates that the typical time needed for a neuron to overcome the threshold and spike again introduces a characteristic scale into the system, entailing periodicity. Observe also that the power spectra exhibit fat tails, with exponent k^{-2}, characteristic of sawtooth profiles with linear increases.

The previous numerical analysis can also be done for the static model, with almost identical results: the origin of the periodic behavior lies in the charging/discharging cycle of potentials, V, and is not crucially affected by the synaptic strengths being fixed or not.

Given that individual neurons oscillate with a certain periodicity, let us study (in analogy with other analyses of non-conserving self-organized systems) the synchronization (or absence of it) between different units (either neurons or synapses).

In order to quantify synchronization, we use bins of size 2×10^{-7} (for V) and 10^{-6} (for J), and consider as an order parameter the fraction of neurons/synapses which are synchronized, i.e. which lie in the same discrete bin, divided by the number of occupied bins. Such a parameter becomes arbitrarily small for a large enough random system and is 1 in the case of perfect synchronization. If the total number of elements in a multiply occupied bin is $N_{\rm s}$ and the number of bins is $N_{\rm b}$, the value of the synchronization order parameter, ϕ, is

$$\phi_V \sim \frac{N_{\rm s}/N}{N_{\rm b}} \qquad \phi_J \sim \frac{N_{\rm s}/N(N-1)}{N_{\rm b}} \tag{A.1}$$

for neurons (V) and synapses (J), respectively. By monitoring ϕ_V, we observe that the potentials in the system converge to a totally unsynchronized state ($\phi_V \sim 10^{-5}$). This is in agreement with the uniform distribution of values of V employed in analytical arguments above.

On the other hand, by measuring ϕ_J we observe that it rapidly converges to a stationary state value, $N_{\rm b} = N$, reflecting a perfect synchronization of the different synapses of any given neuron, j, i.e. $J_{ij} = J_{kj}$ for any values of i and k: *all the*

synapses J_{ij} emerging from of a given (pre-synaptic) neuron, j, converge to a common state. This can be easily understood using the following argument. The dynamics of J_{ij} and $J_{k,j}$ are controlled by the same equation

$$\frac{\partial J_{l,j}}{\partial t} = \frac{1}{\tau_J}\left(\frac{\alpha}{u} - J_{l,j}\right) - uJ_{l,j}\eta(t), \tag{A.2}$$

where l is either i or k and $\eta(t)$ is a (positive) noise, accounting for the spikes of (pre-synaptic) neuron j, which is obviously common to all synapses of j. Subtracting equation (A.2) for k from equation (A.2) for i we obtain that the difference, $\Delta = J_{ij} - J_{kj}$ evolves as

$$\frac{\partial \Delta}{\partial t} = -\Delta\left[\frac{1}{\tau_J} + u\eta(t)\right], \tag{A.3}$$

which, given the positivity of τ_J, u and η, entails a negative Lyapunov exponent and, hence, convergence to the synchronous state, $J_{i,j} = J_{k,j}$—i.e. all synapses emerging from a given pre-synaptic neuron synchronize. Observe that this type of synchronization is similar (but not identical) to that observed in, for instance, earthquake models [43].

References

[1] Bak P, Tang C and Wiesenfeld K, *Self-organized criticality: an explanation of* $1/f$ *noise*, 1987 *Phys. Rev. Lett.* **59** 381
Bak P, 1996 *How Nature Works: The Science of Self-Organized Criticality* (New York: Copernicus)
Jensen H J, 1998 *Self-Organized Criticality* (Cambridge: Cambridge University Press)

[2] Dickman R, Muñoz M A, Vespignani A and Zapperi S, *Paths to self-organized criticality*, 2000 *Braz. J. Phys.* **30** 27

[3] Grinstein G, *Generic scale-invariance and self-organized criticality*, 1995 *Scale-Invariance, Interfaces and Non-Equilibrium Dynamics; Proc. 1994 NATO Adv. Study Inst.* ed A McKane *et al* and references therein
Grinstein G, *Generic scale invariance in classical nonequilibrium systems*, 1991 *J. Appl. Phys.* **69** 5441

[4] Bonachela J A and Muñoz M A, *Self-organization without conservation: true or just apparent scale-invariance?*, 2009 *J. Stat. Mech.* P09009

[5] Beggs J M and Plenz D, *Neuronal avalanches in neocortical circuits*, 2003 *J. Neurosci.* **23** 11167
Beggs J M and Plenz D, *Neuronal avalanches are diverse and precise activity patterns that are stable for many hours in cortical slice cultures*, 2004 *J. Neurosci.* **24** 5216

[6] Beggs J M, *The criticality hypothesis: how local cortical networks might optimize information processing*, 2008 *Phil. Trans. R. Soc.* A **366** 329

[7] Plenz D and Thiagaran T C, *The organizing principles of neural avalanches: cell assemblies in the cortex*, 2007 *Trends Neurosci.* **30** 101

[8] Gireesh E D and Plenz D, *Neural avalanches organize as nested theta-and beta/gamma-oscillations during development of cortical layers*, 2008 *Proc. Nat. Acad. Sci.* **105** 7576
Petermann T, Thiagarajan T A, Lebedev M, Nicolelis M, Chialvo D R and Plenz D, *Spontaneous cortical activity in awake monkeys composed of neuronal avalanches*, 2009 *Proc. Nat. Acad. Sci.* **106** 15921
Priesemann V, Munk M H J and Wibral M, *Subsampling effects in neuronal avalanche distributions recorded in vivo BMC*, 2009 *Neuroscience* **10** 40

[9] Dayan P and Abbott L F, *Theoretical Neuro-science: Computational and Mathematical Modeling of Neural Systems* (Cambridge, MA: MIT Press)
Freeman W J, 2000 *Neurodynamics* (New York: Springer)
Gerstner W and Kistler W, 2002 *Spiking Neuron Models* (Cambridge: Cambridge University Press)
Buzsáki G, 2006 *Rhythms of the Brain* (Oxford: Oxford University Press)

[10] Eckmann J-P, Feinerman O, Gruendlinger L, Moses E, Soriano J and Tlusty T, *The physics of living neural networks*, 2007 *Phys. Rep.* **449** 54

[11] Segev R, Shapira Y, Benveniste M and Ben-Jacob E, *Observation and modeling of synchronized bursting in two dimensional neural network*, 2001 *Phys. Rev.* E **64** 011920

J. Stat. Mech. (2010) P02015

Segev R *et al*, *Long term behavior of lithographically prepared in vitro neuronal networks*, 2002 *Phys. Rev. Lett.* **88** 118102
Segev R, Baruchi I, Hulata E and Ben-Jacob E, *Hidden neuronal correlations in cultured networks*, 2004 *Phys. Rev. Lett.* **92** 118102
[12] Ikegaya Y *et al*, *Synfire chains and cortical songs: temporal modules of cortical activity*, 2003 *Science* **304** 559
[13] Eytan D and Marom S, *Dynamics and effective topology underlying synchronization in networks of cortical neurons*, 2006 *J. Neurosci.* **26** 8465
[14] van Pelt J *et al*, *Characterization of firing dynamics of spontaneous bursts in cultured neural networks*, 2005 *IEEE Trans. Biomed. Eng.* **51** 2051
[15] Wagenaar D A, Nadasdy Z and Potter S M, *Persistent dynamic attractors in activity patterns of cultured neural networks*, 2006 *Phys. Rev.* E **73** 051907
[16] Herz A V M and Hopfield J J, *Earthquake cycles and neural reverberations: collective oscillations in systems with pulse-coupled threshold elements*, 1995 *Phys. Rev. Lett.* **75** 1222
[17] Markram H and Tsodyks M, *Redistribution of synaptic efficacy between neocortical pyramidal neurons*, 1996 *Nature* **382** 807
[18] Dorogovtsev S N, Goltsev A V and Mendes J F F, *Critical phenomena in complex networks*, 2008 *Rev. Mod. Phys.* **80** 1275
[19] Shefi O, Golding I, Segev R, Ben-Jacob E and Ayali A, *Morphological characterization of in vitro neuronal networks*, 2002 *Phys. Rev.* E **66** 021905
Pajevic S and Plenz D, *Efficient network reconstruction from dynamical cascades identifies small-world topology of neuronal avalanches*, 2008 *PLoS Comp. Biol.* **5** e1000271
[20] Albert R and Barabási A-L, *Statistical mechanics of complex networks*, 2002 *Rev. Mod. Phys.* **74** 47
[21] Harris T E, 1989 *The Theory of Branching Processes* (New York: Dover)
[22] Hadelman C and Beggs J M, *Critical branching captures activity in living neural networks and maximizes the number of metastable states*, 2005 *Phys. Rev. Lett.* **94** 058101
[23] Hsu D and Beggs J M, *Neuronal avalanches and criticality: a dynamical model for homeostasis*, 2006 *Neurocomputing* **69** 1134
[24] Legenstein R and Maas W, *Edge of chaos and prediction of computational performance for neural circuit models*, 2007 *Neural Networks* **20** 323
[25] Bertschinger N and Natschlager T, *Real-time computation at the edge of chaos in recurrent neural networks*, 2004 *Neural Comput.* **16** 1413
[26] Kinouchi O and Copelli M, *Optimal dynamical range of excitable networks at criticality*, 2006 *Nat. Phys.* **2** 348
Chialvo D, *Are our senses critical*, 2006 *Nat. Phys.* **2** 301
[27] Bédard C, Kröger H and Destexhe A, *Does the* $1/f$ *frequency scaling of brain signals reflect self-organized critical states?*, 2006 *Phys. Rev. Lett.* **97** 118102
[28] Pasquale V, Massobrio P, Bologna L L, Chiappalone M and Martinoia M, *Self-organization and neural avalanches in networks of dissociated cortical neurons*, 2008 *Neuroscience* **153** 1354
[29] Levina A, Herrmann J M and Geisel T, *Dynamical synapses causing self-organized criticality in neural networks*, 2007 *Nat. Phys.* **3** 857
[30] Halley J D and Wrinkler D A, *Critical-like self-organization and natural selection: two facets of a single evolutionary process?*, 2009 *BioSystems* **92** 148
[31] Royer S and Paré D, *Conservation of total synaptic weight through balanced synaptic depression and potentiation*, 2003 *Nature* **422** 518
[32] Persi E, Horn D, Segev R, Ben-Jacob E and Volman V, *Modeling of synchronization of bursting events: The importance of inhomogeneity*, 2004 *Neurocomputing* **58** 179
[33] Levina A, Herrmann J M and Geisel T, *Phase transitions towards criticality in a neural system with adaptive interactions*, 2009 *Phys. Rev. Lett.* **102** 118110
[34] Eurich C W, Herrmann J M and Ernst U A, *Finite-size effects of avalanche dynamics*, 2002 *Phys. Rev.* E **66** 066137
Levina A, Herrmann J M and Geisel T, *Dynamical synapses give raise to a power-law distribution of neuronal avalanches*, 2006 *Advances in Neural Information Processing Systems* vol 18, ed Y Weiss, B Schölkopf and J Platt (Cambridge, MA: MIT Press) p 771
Levina A, Ernst U and Herrmann J M, *Criticality of avalanche dynamics in adaptive recurrent networks*, 2007 *Neurocomputing* **70** 1877

J. Stat. Mech. (2010) P02015

[35] Bröker H-M and Grassberger P, *Random neighbor theory of the Olami–Feder–Christensen earthquake model*, 1997 *Phys. Rev.* E **56** 3944
Pruessner G and Jensen H J, *A solvable non-conservative model of self-organised criticality*, 2002 *Europhys. Lett.* **58** 250
Chabanol M L and Hakim V, *Analysis of a dissipative model of self-organized criticality with random neighbors*, 1997 *Phys. Rev.* E **56** R2343
[36] Pantic L, Torres J J, Kappen H J and Gielen S C A M, *Associative memory with dynamic synapses*, 2002 *Neural Comput.* **14** 2903
[37] See, for instance Hennig M H, Adams C, Willshaw D and Sernagor E, *Early-stage waves in the retinal network emerge close to a critical state transition between local and global functional connectivity*, 2009 *J. Neurosci.* **29** 1077
[38] Athreya K B and Karlin S, *Branching processes with random environments*, 1970 *Bull. Amer. Math. Soc.* **76** 865
Smith W and Wilkinson W, *On branching processes in random environments*, 1969 *Ann. Math. Statist.* **40** 814
[39] Vespignani A, Dickman R, Muñoz M A and Zapperi S, *Driving, conservation and absorbing states in sandpiles*, 1998 *Phys. Rev. Lett.* **81** 5676
Vespignani A, Dickman R, Muñoz M A and Zapperi S, *Absorbing phase transitions in fixed-energy sandpiles*, 2000 *Phys. Rev.* E **62** 4564
Dickman R, Alava M, Muñoz M A, Peltola J, Vespignani A and Zapperi S, *Critical behavior of a one-dimensional stochastic sandpiles*, 2001 *Phys. Rev.* E **64** 056104
Muñoz M A, Dickman R, Vespignani A and Zapperi S, *Avalanche and spreading exponents in systems with absorbing states*, 1999 *Phys. Rev.* E **59** 6175
Alava M and Muñoz M A, *Interface depinning versus absorbing state transitions*, 2002 *Phys. Rev.* E **65** 026145
[40] Bonachela J A, Ramasco J J, Chaté H, Dornic I and Muñoz M A, *Sticky grains do not change the universality of isotropic sandpiles*, 2006 *Phys. Rev.* E **74** 050102(R)
Bonachela J A, Chaté H, Dornic I and Muñoz M A, *Absorbing States and elastic interfaces in random media: two equivalent descriptions of self-organized criticality*, 2007 *Phys. Rev. Lett.* **98** 155702
Bonachela J A and Muñoz M A, *Confirming and extending the hypothesis of sandpile universality*, 2008 *Phys. Rev.* E **78** 041102
[41] Cardy J L and Grassberger P, *Epidemic models and percolation*, 1985 *J. Phys. A: Math. Gen.* **18** L267
Janssen H K, *Renormalized field theory of dynamical percolation*, 1985 *Z. Phys.* B **58** 311
[42] de Arcangelis L, Perrone-Capano C and Herrmann H J, *Self-organized criticality model for brain plasticity*, 2006 *Phys. Rev. Lett.* **96** 028107
[43] Grassberger P, *Efficient large-scale simulations of a uniformly driven system*, 1994 *Phys. Rev.* E **49** 2436
Middleton A A and Tang C, *Self-organized criticality in nonconserved systems*, 1995 *Phys. Rev. Lett.* **74** 742
Corral A, Pérez C J, Díaz-Guilera A and Arenas A, *Self-organized criticality and synchronization in a lattice model of integrate-and-fire oscillators*, 1995 *Phys. Rev. Lett.* **74** 118
Kotani T, Yoshino H and Kawamura H, *Periodicity and criticality in the Olami–Feder–Christensen model of earthquakes*, 2008 *Phys. Rev.* E **77** 010102(R)

J. Stat. Mech. (2010) P02015